ACS Sustainable Chemistry & Engineering

Research Article

pubs.acs.org/journal/ascecg

# Carbon Dioxide Sequestration: Influence of Porous Media on Hydrate Formation Kinetics

Gaurav Bhattacharjee, Asheesh Kumar, Tushar Sakpal, and Rajnish Kumar*

Chemical Engineering and Process Development Division, National Chemical Laboratory, Dr. Homi Bhabha Road, Pune 411 008, India

Supporting Information

**ABSTRACT:** In the present study, $CO_2$ sequestration by hydrate formation in porous sediments has been discussed. Two siliceous materials with high porosities, pumice and fire hardened red clay (FHRC), have been used as packing materials in a fixed bed setup to study hydrate formation kinetics. The results obtained using the aforementioned materials were compared with those obtained using silica sand and quartz. Carbon dioxide hydrate formation kinetics was studied at 3.0 MPa pressure and 274 K temperature. Two different types of experiments were conducted: (a) using a constant volume of water and (b) maintaining a constant bed height. These experiments were conducted using the different porous media individually as packing materials. It was observed that pumice as the porous medium showed better hydrate formation kinetics resulting in 46 mol % water to hydrate conversion in 5 h. Moreover, kinetics was enhanced with decrease in the bed height of pumice; this suggests that at field scale adaptation of $CO_2$ sequestration in geological formations, mass transfer limitations would be significant. The effects of particle size on hydrate formation kinetics were also investigated. It was observed that hydrate formation kinetics was enhanced with decrease in the particle size fraction.

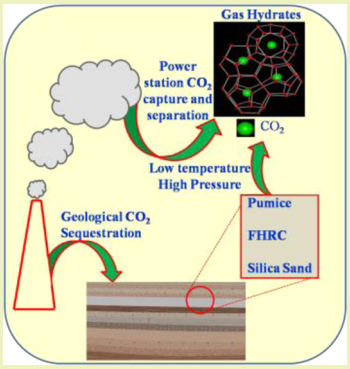


**KEYWORDS:** *Gas hydrate, Particle size, Gas uptake, Geological sequestration, Bed height*

## INTRODUCTION

Carbon dioxide, a major greenhouse gas, is an undesirable byproduct of energy related activities such as electricity generation from fossil fuel combustion.[1−3] Efficient capture and storage of $CO_2$ is pegged as a short- to medium-term solution to contain the anthropogenic release of $CO_2$ into the atmosphere. $CO_2$ capture and separation from a gas mixture can be achieved through several approaches. These include conventional approaches like ethanol amine based chemical absorption process, pressure and temperature swing adsorption process, membrane separation and Solexol/Rectisol based physical absorption process. Some unconventional processes for $CO_2$ capture (which are still in development stage) are use of metal organic frameworks and ionic liquids for preferential $CO_2$ adsorption through weak chemical forces. The hydrate based gas separation (HBGS) process is one such technology that can preferentially adsorb $CO_2$ through enclathration of $CO_2$ in ice like cages.[4−6] Gas hydrates (GHs) are crystalline compounds formed through the interaction of hydrogen bonded host (water) molecules and small guest molecules at suitable pressure and temperature conditions.[7] GHs find applications in gas capture and storage, gas transport and seawater desalination. However, the most important reason for studying gas hydrate is assessment and exploitation of naturally occurring methane GHs, which are considered to be a vast, untapped source of energy.[4,8−14]

Carbon dioxide sequestration is defined as storage of anthropogenic $CO_2$ in geological formations either permanently or for geologically significant time periods.[14−20] Depleted oil and gas reservoirs, saline aquifers, unmineable coal beds and deep sea beds are geological formations that can be used for long-term $CO_2$ sequestration. Another option of deep ocean storage is plagued by environmental concerns such as ocean acidification and eutrophication.[21] In Canada, about 5 Mt of acid gases ($CO_2$ and $H_2S$) have been safely stored into depleted gas reservoirs. The Sleipner West gas field in the North Sea is another example of underground $CO_2$ storage in porous sediment.[16,18] The above studies all refer to $CO_2$ storage in the fluid phase. Site selection for $CO_2$ storage needs addressing of various factors such as appropriate porosity and permeability of the reservoir rock, temperature, pressure and the availability of a stable geological environment.[21] $CO_2$ storage in the form of solid hydrates in underground reservoirs is promising as 1 $m^3$ of $CO_2$ hydrate can store 120−160 $m^3$ of $CO_2$ gas at STP.[14,16,22] Sun and Englezos mimicked the conditions of the depleted gas reservoir at Northern Alberta, Canada. The objective was to assess the potential of the site in question to serve as a host for $CO_2$ storage in the form of solid hydrates.[14]

India has a complex and diverse geology. Much of the geology of present-day India is a result of volcanic eruptions dating back to prehistoric eras. The Indian subcontinent is mantled with the remnants of at least five continental flood

Received: March 4, 2015
Revised: April 17, 2015
Published: April 24, 2015




DOI: 10.1021/acssuschemeng.5b00171
ACS Sustainable Chem. Eng. 2015, 3, 1205−1214

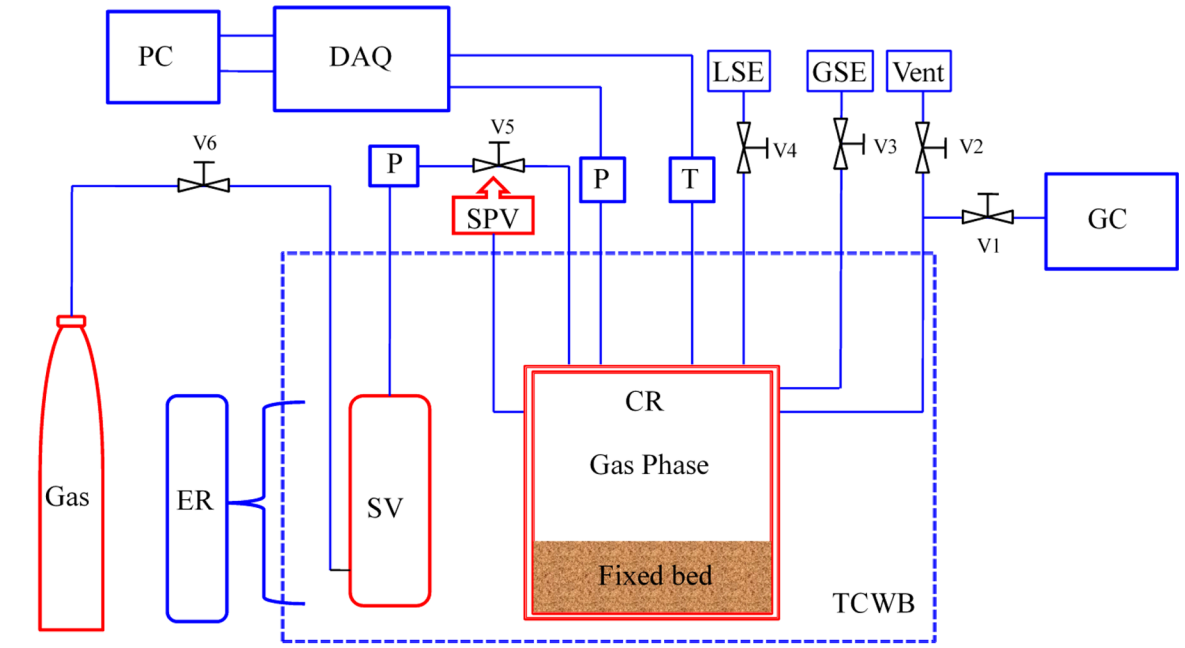


| | | | |
|---|---|---|---|
| CR | Crystallizer | DAQ | Data Acquisition System |
| SV | Supply Vessel | ER | External Refrigerator |
| GC | Gas Chromatography | SPV | Safety Pressure Valve |
| P | Pressure Transducer | GSE | Gas sample extraction |
| T | Thermocouples | LSE | Liquid sample extraction |
| TCWB | Temperature Controlled Water Bath | | |

**Dimensions of Important Components:**

**1) CR:** I.D.: 6.4 cm
O.D.: 8.5 cm
Depth: 10.1 cm

**2) SV:** Volume: 300 $cm^3$

**3) TCWB:** Length: 30 cm
Breadth: 24 cm
Depth: 15 cm

**Figure 1.** Schematic of the experimental apparatus.

basalt provinces that occurred between the middle Proterozoic to the late Cretaceous-early Tertiary eras.[23] The geographical land area of India can be divided into three parts: The Deccan Trap (youngest of the five continental flood basalt provinces), Gondwana and Vindhayan.[24] The Deccan Trap is acknowledged to be one of the largest volcanic features on Earth. It presently occupies around half a million square kilometers of western and central India and southernmost Pakistan.[23] The rocks found in the Deccan Trap are mainly igneous type (formed through the cooling and solidification of magma or lava).[23−25] To simulate such lithography in a laboratory setup for studying $CO_2$ hydrate formation kinetics, we have chosen pumice and fire hardened red clay (FHRC) with suitable water saturation. Hydrate formation kinetics are studied in these two media and the results are compared with those obtained using silica sand and quartz. Pumice and FHRC are both highly siliceous materials with much higher porosities as compared to silica sand and quartz. Silica sand and quartz are porous sediments found in depleted oil and gas reservoirs. Unfortunately, India does not have many depleted oil and gas reserves. Thus, a comparison study on $CO_2$ hydrate formation kinetics using siliceous volcanic materials such as pumice and FHRC (a model material), which are available in plenty in the Indian subcontinent, is going to be valuable in assessing the feasibility of sequestering $CO_2$ in the form of hydrates for the same.

Pumice is a volcanic rock with an unusual foamy configuration that is created when superheated, highly pressurized rock is violently ejected from a volcano.[26,27] On land, it can be found anywhere in the vicinity of a volcano. It can also be found floating in the sea, attributable to underwater volcanoes ejecting molten lava and volcanic gases well above sea level. When the molten lava comes in contact with cold seawater, it hardens to form pumice. FHRC, which is used in the construction industry, is used as a model material in this work, as it closely mimics the nature of siliceous volcanic deposits. Pumice and FHRC both mainly consist of $SiO_2$ and $Al_2O_3$ with varying amounts of other materials such as magnesia, iron oxide, lime, etc.[28−30] Like pumice, FHRC is also created at conditions of high pressure and temperature, around 900−1000 °C.[31] The conditions of formation of these


DOI: 10.1021/acssuschemeng.5b00171
ACS Sustainable Chem. Eng. 2015, 3, 1205−1214

Table 1. Summary of All Experiments Conducted with Constant Volume of Water (24 mL)[a]

| system | average porosity (vol %) ± SD | vol. of water used ($cm^3$) | bed height (cm) | exp. no. | run type | gas consumed (mol of gas/mol of water) | final water to hydrate conversion (mol %) | final gas to hydrate conversion (mol %) | induction time (min) | average induction time ± SD |
|---|---|---|---|---|---|---|---|---|---|---|
| sand size: 30−400 μm | 30.7 ± 0.8 | 24.0 | 3.0 | 1 | fresh | 0.040 | 23.1 | 14.5 | 9.0 | 18.6 ± 15.6 |
| | | | | 2 | repeat | 0.040 | 23.1 | 14.9 | 10.8 | |
| | | | | 3 | fresh | 0.051 | 29.3 | 19.7 | 5.4 | |
| | | | | 4 | repeat | 0.064 | 36.8 | 25.3 | 26.0 | |
| | | | | 5 | fresh | 0.044 | 25.1 | 16.1 | 3.0 | |
| | | | | 6 | repeat | 0.076 | 44.1 | 31.2 | 31.3 | |
| | | | | 7 | repeat | 0.067 | 38.4 | 24.8 | 44.5 | |
| quartz size: 200−1000 μm | 24.0 ± 0.7 | 24.0 | 4.5 | 8 | fresh | 0.033 | 19.1 | 14.1 | 0.3 | 7.4 ± 8.8 |
| | | | | 9 | repeat | 0.034 | 19.8 | 14.4 | 0.2 | |
| | | | | 10 | repeat | 0.041 | 23.0 | 17.6 | 6.2 | |
| | | | | 11 | fresh | 0.031 | 18.3 | 13.8 | 1.1 | |
| | | | | 12 | repeat | 0.042 | 24.1 | 18.3 | 16.9 | |
| | | | | 13 | repeat | 0.038 | 21.9 | 17.1 | 19.8 | |
| pumice size: >420 μm | 46.4 ± 2.0 | 24.0 | 2.2 | 14 | fresh | 0.024 | 13.6 | 7.4 | 5.3 | 32.1 ± 24.0 |
| | | | | 15 | repeat | 0.019 | 10.7 | 6.5 | 39.7 | |
| | | | | 16 | repeat | 0.018 | 10.4 | 6.5 | 51.3 | |
| pumice size: 210−420 μm | 57.0 ± 1.8 | 24.0 | 2.3 | 17 | fresh | 0.050 | 29.0 | 15.9 | 1.8 | 10.3 ± 9.8 |
| | | | | 18 | repeat | 0.066 | 37.7 | 21.1 | 8.2 | |
| | | | | 19 | repeat | 0.032 | 18.5 | 10.3 | 21.1 | |
| pumice size: <210 μm | 42.3 ± 0.7 | 24.0 | 2.7 | 20 | fresh | 0.080 | 46.0 | 26.4 | 10.3 | 31.6 ± 21.5 |
| | | | | 21 | repeat | 0.079 | 45.1 | 26.5 | 48.5 | |
| | | | | 22 | repeat | 0.082 | 47.1 | 27.7 | 47.8 | |
| | | | | 23 | fresh | 0.084 | 48.2 | 27.2 | 0.2 | |
| | | | | 24 | repeat | 0.072 | 41.3 | 24.7 | 49.5 | |
| | | | | 25 | fresh | 0.074 | 42.3 | 24.2 | 17.1 | |
| FHRC size: >420 μm | 31.2 ± 1.7 | 24.0 | 3.5 | 26 | fresh | 0.025 | 14.3 | 9.3 | 6.3 | 71.1 ± 62.9 |
| | | | | 27 | repeat | 0.022 | 12.7 | 8.3 | 75.0 | |
| | | | | 28 | repeat | 0.020 | 11.9 | 7.9 | 131.9 | |
| FHRC size: 210−420 μm | 49.0 ± 2.9 | 24.0 | 2.4 | 29 | fresh | 0.039 | 22.2 | 12.6 | 1.8 | 93.4 ± 144.8 |
| | | | | 30 | repeat | 0.034 | 19.8 | 11.3 | 18.0 | |
| | | | | 31 | repeat | 0.029 | 16.6 | 9.6 | 260.4 | |
| FHRC size: <210 μm | 55.9 ± 2.0 | 24.0 | 2.4 | 32 | fresh | 0.065 | 37.5 | 21.0 | 0.2 | 61.6 ± 87.9 |
| | | | | 33 | repeat | 0.061 | 35.1 | 20.0 | 115.0 | |
| | | | | 34 | repeat | 0.059 | 34.0 | 19.5 | 216.4 | |
| | | | | 35 | fresh | 0.076 | 43.7 | 23.8 | 0.1 | |
| | | | | 36 | repeat | 0.062 | 35.9 | 20.6 | 36.4 | |
| | | | | 37 | fresh | 0.066 | 37.9 | 21.4 | 1.3 | |

[a]The dependent variables listed are bed height, induction time, the amount of $CO_2$ gas consumed until the end of the reaction, the water to hydrate conversion and the gas ($CO_2$) to hydrate conversion. Experimental temperature and pressure were 274 K and 3.0 MPa, respectively. The gas uptake was measured for a fixed time of 5 h after induction for all the experiments conducted.

two materials tell us that these are geologically stable formations. The Deccan Trap abounds with highly siliceous volcanic rocks like pumice.[23,25] The Central Indian Basin (CIB) is another volcanic province that consists of layers of ash and pumice.[32,33] The volcanic islands: Narcondam and Barren Island (India's only active volcano) in the Andamans are also sources of pumice and similar volcanic rocks such as scoria.[34]

All the four porous materials discussed above have potential for use as porous geological media for $CO_2$ storage. In the present work, the effects of these porous materials on hydrate formation kinetics were studied and compared. Three different size fractions were made for (a) pumice and (b) FHRC. Two types of experiments were conducted: first, the volume of water used was kept constant leading to different bed heights and second, the bed height was kept constant resulting in different volumes of water used in each case.

## EXPERIMENTAL SECTION

**Materials.** Carbon dioxide gas with a certified purity of more than 99.9% was supplied by Vadilal Gases Ltd., India. Silica sand and Quartz used in this study were purchased from Sakalchand & Company, Pune, India. The volume of water required to completely fill the void space between the sand particles and quartz particles was 0.20 and 0.16 $cm^3$/g, respectively.[35] Pumice and FHRC were purchased from Pune, India. The pumice and FHRC samples were ground to different size fractions: (a) less than 210 μm, (b) 210−420 μm and (c) more than 420 μm. The volume of water required to completely fill the void interstitial spaces between the particles of different size fractions of pumice and FHRC are included in the Supporting Information as Table S1.

**Apparatus and Procedure for Hydrate Formation Experiment.** A detailed description and schematic of the fixed bed apparatus, as shown in Figure 1, has been given in Kumar et.al.[36] The procedure for the hydrate formation experiments is as follows. For each of the four porous media discussed above, two types of experiments were carried out: (a) with a constant volume of water (24 $cm^3$) and varying bed heights (Table 1) and (b) with a constant bed height (3 cm) and


DOI: 10.1021/acssuschemeng.5b00171
ACS Sustainable Chem. Eng. 2015, 3, 1205−1214

**Table 2. Summary of All Experiments Conducted with Constant Bed Height (3 cm)[a]**

| system | average porosity (vol %) ± SD | volume of water used ($cm^3$) | bed height (cm) | exp. no | run type | carbon dioxide consumed (mol of gas/mol of water) | final water to hydrate conversion (mol %) | final gas to hydrate conversion (mol %) | induction time (min) | average induction time ± SD |
|---|---|---|---|---|---|---|---|---|---|---|
| sand size: 30−400 μm | 30.6 ± 0.8 | 24.0 | 3.0 | | | | as given in Table 1 | | | |
| quartz size: 200−1000 μm | 24.0 ± 0.7 | 16.5 | 3.0 | 38 | fresh | 0.016 | 15.4 | 6.3 | 0.3 | 6.2 ± 9.1 |
| | | | | 39 | repeat | 0.039 | 22.2 | 9.4 | 0.5 | |
| | | | | 40 | repeat | 0.042 | 24.2 | 9.9 | 0.5 | |
| | | | | 41 | fresh | 0.027 | 15.4 | 6.4 | 0.2 | |
| | | | | 42 | repeat | 0.047 | 26.8 | 11.2 | 16.2 | |
| | | | | 43 | repeat | 0.045 | 25.6 | 10.8 | 19.7 | |
| pumice size: <210 μm | 42.3 ± 0.7 | 25.5 | 3.0 | 44 | fresh | 0.084 | 48.2 | 31.8 | 5.5 | 99.5 ± 199.5 |
| | | | | 45 | repeat | 0.062 | 37.7 | 27.9 | 39.0 | |
| | | | | 46 | repeat | 0.060 | 35.6 | 26.7 | 40.5 | |
| | | | | 47 | fresh | 0.071 | 41.0 | 27.8 | 22.0 | |
| | | | | 48 | repeat | 0.061 | 34.7 | 24.9 | 28.8 | |
| | | | | 49 | repeat | 0.062 | 35.1 | 26.0 | 551.0 | |
| | | | | 50 | fresh | 0.068 | 38.8 | 25.8 | 10.0 | |
| FHRC size: <210 μm | 55.9 ± 2.0 | 28.3 | 3.0 | 51 | fresh | 0.072 | 41.6 | 29.5 | 0.3 | 115.1 ± 189.9 |
| | | | | 52 | repeat | 0.058 | 33.1 | 24.9 | 60.0 | |
| | | | | 53 | fresh | 0.073 | 41.7 | 29.4 | 0.2 | |
| | | | | 54 | repeat | 0.057 | 32.6 | 24.4 | 485.0 | |
| | | | | 55 | fresh | 0.068 | 39.0 | 27.4 | 0.2 | |
| | | | | 56 | repeat | 0.059 | 34.0 | 25.2 | 145.0 | |

[a]The dependent variables listed are volume of water used, induction time, the amount of $CO_2$ gas consumed until the end of the reaction, the water to hydrate conversion and the gas ($CO_2$) to hydrate conversion. Experimental temperature and pressure were 274 K and 3.0 MPa, respectively. The gas uptake was measured for a fixed time of 5 h after induction for all the experiments conducted.



DOI: 10.1021/acssuschemeng.5b00171
ACS Sustainable Chem. Eng. 2015, 3, 1205−1214

**Table 3. Pumice: Effect of Bed Height: Summary of All Experiments Conducted[a]**

| system | average porosity (vol %) ± SD | volume of water used ($cm^3$) | bed height (cm) | exp. no. | run type | carbon dioxide consumed (mol of gas/mol of water) | final gas to hydrate conversion (mol %) | final gas to hydrate conversion (mol %) | induction time (min) | average induction time ± SD |
|---|---|---|---|---|---|---|---|---|---|---|
| pumice size: <210 μm | 42.3 ± 0.7 | 24.0 | 2.7 | as given in Table 1 | | | | | | |
| pumice size: <210 μm | | 44.1 | 5.5 | 57 | fresh | 0.045 | 25.7 | 41.6 | 6.5 | 60.1 ± 59.8 |
| | | | | 58 | repeat | 0.040 | 23.2 | 39.5 | 126.6 | |
| | | | | 59 | repeat | 0.040 | 23.2 | 39.9 | 94.7 | |
| | | | | 60 | fresh | 0.047 | 27.2 | 43.6 | 1.4 | |
| | | | | 61 | repeat | 0.041 | 23.8 | 40.7 | 120.2 | |
| | | | | 62 | fresh | 0.047 | 26.7 | 43.7 | 11.4 | |

[a]The dependent variables listed are bed height, volume of water used, induction time, the amount of $CO_2$ gas consumed until the end of the reaction, the water to hydrate conversion and the gas ($CO_2$) to hydrate conversion. Experimental temperature and pressure were 274 K and 3.0 MPa, respectively. The gas uptake was measured for a fixed time of 5 h after induction for all the experiments conducted.

varying corresponding volumes of water (Table 2). The water saturation of the porous fixed bed was kept constant at 75% for all the experiments conducted in this study. Distilled and deionized water was used. The water saturated packing medium was placed inside a 323 $cm^3$ SS-316 crystallizer (Parr make) that was then firmly sealed and placed inside a temperature controlled water bath in order to attain the desired experimental temperature (274 K). The vessel was flushed with pure $CO_2$ gas using a supply vessel by repeating rapid pressurization (~0.5 MPa) and depressurization cycles. Next, the crystallizer was pressurized with pure $CO_2$ gas up to a predetermined experimental pressure of 3.0 MPa (equilibrium hydrate formation pressure for pure $CO_2$ gas at 274 K is 1.509 MPa),[7] thus providing sufficient driving force for the hydrate formation reaction. At this stage, gas uptake measurements were initiated that were all performed in batch mode with pure $CO_2$ gas at a constant temperature of 274 K. Hydrate formation is accompanied by pressure drop inside the vessel as a result of the gas moving from the gas phase into the solid hydrate phase. This drop in pressure, measured employing a pressure transducer (WIKA make; range: 0–25 MPa) was used to calculate the moles of gas participating in the hydrate formation experiment. Temperature and pressure inside the vessel were recorded every 5 s using a data acquisition system (PPI, Mumbai, India). As entire experiments were conducted in batch mode, the effective driving force for hydrate formation decreased as the reaction proceeded with more and more $CO_2$ gas moving from the gas phase to the solid hydrate phase.

**Calculation of the Amount of Gas Consumed during the Hydrate Formation Experiments.** At any given time, the total number of moles of gas that was consumed in the hydrate formation process is the difference between the number of moles of gas present in the gas phase of the crystallizer at time $t = 0$ and the number of moles of gas present in the gas phase of the crystallizer at time $t = t$. The same is given by the following equation:[37]

$$(\Delta n_{H,\downarrow})_t = V_{CR}\left[\frac{P}{zRT}\right]_0 - V_{CR}\left[\frac{P}{zRT}\right]_t \quad (1)$$

where $z$ is the compressibility factor calculated by Pitzer's correlation;[38] $V_{CR}$ is the volume of the gas phase inside the crystallizer. $P$ and $T$ are the pressure and temperature of the crystallizer.

**Calculation of the Water to Hydrate Conversion.** The amount of water that was converted to hydrate was determined by using the following equation:[37]

$$\text{conversion of water to hydrate (mol\%)} = \frac{\Delta n_{H,\downarrow} \times \text{hydration no.}}{n_{H_2O}} \times 100 \quad (2)$$

where $\Delta n_{H,\downarrow}$ is the total number of moles of gas consumed at the end of the hydrate formation process as calculated from the gas uptake measurements and $n_{H_2O}$ is the total number of moles of water in the system. The hydration number used for the above calculations is 5.75.[7]

**Calculation of the $CO_2$ to Hydrate Conversion.** The amount of gas ($CO_2$) that was converted to hydrate was determined by using the following equation:[39]

$$\text{conversion of } CO_2 \text{ to hydrate (mol\%)} = \frac{(\Delta n_{H,\downarrow})}{(n_{start} - n_{eqbm})} \times 100 \quad (3)$$

where $\Delta n_{H,\downarrow}$ is the total number of moles of gas consumed at the end of the hydrate formation process as calculated from the gas uptake measurements, $n_{start}$ is the number of moles of gas present in the gas phase of the system at the start of the experiment and $n_{eqbm}$ is the number of moles of gas present in the gas phase of the system at equilibrium ($P$ and $T$).

**Calculation of the Hydrate Saturation.** The $CO_2$ hydrate saturation was calculated using the following equation:[14]

$$\text{hydrate saturation (\%)} = (\text{initial water saturation} \times \text{water to hydrate conversion} \times 1.1) \quad (4)$$

The density of $CO_2$ hydrate being less than that of water, when water is converted into hydrate, the volume of the hydrate phase is taken to be 1.1 times that of the originally existing water.[14]

**Calculation of the Rate of Hydrate Formation.** The rate of hydrate formation was calculated by the forward difference method as given below:[37]

$$\left(\frac{d\Delta n_{H,\downarrow}}{dt}\right)_t = \frac{\Delta n_{H,\downarrow(t+\Delta t)} - \Delta n_{H,\downarrow(t)}}{\Delta t}; \quad \Delta t = 5 \text{ s} \quad (5)$$

The average of these rates was calculated for every 20 min and reported.

## RESULTS AND DISCUSSIONS

Tables 1, 2 and 3 summarize all the relevant information for each experiment conducted during this study. These include the sample state, the volume of water used, the bed height, induction times, the amount of gas consumed, the water to hydrate conversion in mol % and the gas to hydrate conversion in mol %. Hydrate formation was investigated for a fixed time of 5 h after nucleation for all the experiments conducted. The reason for choosing 5 h as the cutoff point for studying hydrate formation is that the overall conclusion would not change even if the study would be extended for another 5 h. Figure S1 in the Supporting Information shows the hydrate formation kinetics for each of the four systems for at least 12 h from nucleation.

Hydrate formation kinetics are usually discussed through a gas uptake curve. A typical gas uptake curve for hydrate formation can be divided into three parts. First is the dissolution stage during which the gas gets dissolved into the



DOI: 10.1021/acssuschemeng.5b00171
ACS Sustainable Chem. Eng. 2015, 3, 1205–1214

system. The next stage is the hydrate nucleation. The hydrate nucleation phenomenon continues until the formation of critical sized stable hydrate nuclei. Once nucleation occurs, we enter the hydrate growth phase where the formed hydrate nuclei grow as solid hydrate particles.[40] The average induction times along with standard deviation for the hydrate formation experiments in the presence of all the four porous media have been listed in Tables 1, 2 and 3. An illustration of the same has been included in the Supporting Information as Figure S2.

**Gas Hydrate Formation in Various Porous Media with Constant Volume of Water and with Constant Bed Height.** Figures 2 and 3 compare averages of the gas uptake and water to hydrate conversion for the hydrate growth experiments conducted in different porous media (pumice, FHRC, silica sand and quartz). Only the fresh runs have been included in Figures 2 and 3. Figure 2 corresponds to the constant volume of water experiments whereas Figure 3 covers the constant bed height experiments. Time zero in the graphs corresponds to the hydrate nucleation point for the experiments. As seen in Figure 2, hydrate growth kinetics is the best in case of pumice (~46% in 5 h) followed by FHRC, silica sand and quartz, respectively. This can be attributed to two main reasons: First is the effect of particle size. Hydrate formation kinetics is enhanced with decrease in particle size.[41,42] This topic has been discussed in detail later. In the case of both pumice and FHRC, the particle size used is <210 $\mu$m whereas for silica sand and quartz, the particle sizes vary between 30 and 400 $\mu$m and 200−1000 $\mu$m, respectively. This shows that smaller particle size of pumice and FHRC had positive effect on hydrate formation kinetics. The second cause for pumice showing better hydrate formation kinetics is the higher porosity of pumice bed compared to other media. A highly porous bed ensures that for same amount of water used for hydrate formation, it has a smaller bed height compared to others, resulting in better gas−water contact.[12] In the case of the constant bed height experiments that have been highlighted in Figure 3, the bed height is the same in all the cases, and thus the volume of water used varies. As expected, pumice and FHRC again show enhanced hydrate formation kinetics as compared to silica sand and quartz. Averages of the gas uptake and water to hydrate conversion for the repeat runs have been shown in the Supporting Information as Figures S3 and S4, respectively. Rates of gas uptake (mol of gas/mol of water/h) corresponding to Figures 2 and 3 have been plotted against time and are included in the Supporting Information as Figures S5 and S6. Results follow the same trend for both types of experiments: pumice showing the best kinetics followed by FHRC, silica sand and quartz, respectively.

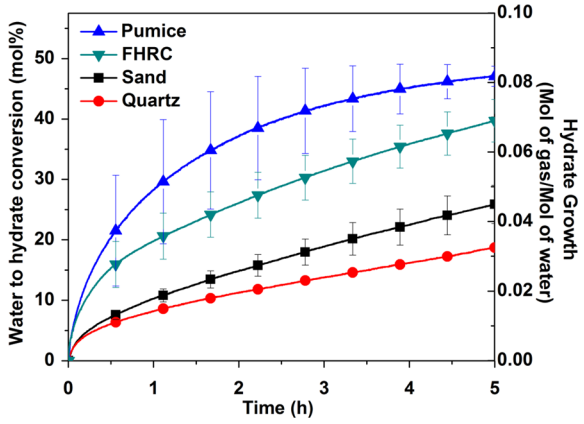


**Figure 2.** Comparison of the gas uptake and water to hydrate conversion in the presence of the different porous media used for the case of the constant volume of water experiments: sand, average and standard deviation of experiment numbers 1, 3 and 5; quartz, average and standard deviation of experiment numbers 8 and 11; pumice, average and standard deviation of experiment numbers 20, 23 and 25; FHRC, average and standard deviation of experiment numbers 32, 35 and 37.

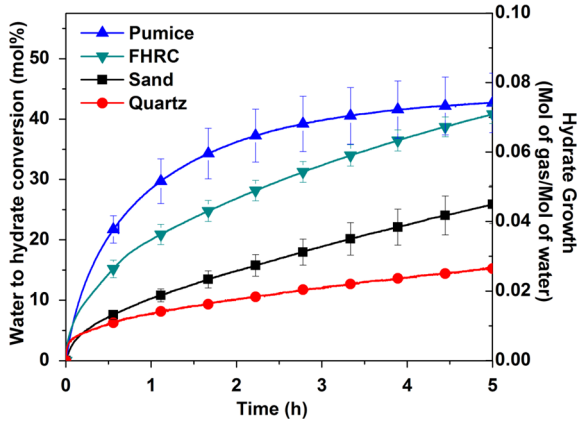


**Figure 3.** Comparison of the gas uptake and water to hydrate conversion in the presence of the different porous media used for the case of the constant bed height experiments: sand, average and standard deviation of experiment numbers 1, 3 and 5; quartz, average and standard deviation of experiment numbers 38 and 41; pumice, average and standard deviation of experiment numbers 44, 47 and 50; FHRC, average and standard deviation of experiment numbers 51, 53 and 55.

**Effect of Particle Size and Water Saturation on Gas Hydrate Formation Kinetics.** The effect of particle size distribution of the porous medium being used, on hydrate formation kinetics, has not been widely studied. Some studies using $CH_4$ and $CO_2$ as the hydrate forming guests have concluded that particle size distribution does affect hydrate formation kinetics.[41−44] Figures 4 and 5 represent the effect of particle size on the hydrate formation kinetics using pumice and FHRC individually as porous media. For the experiments conducted, the figures plot the gas uptake and water to hydrate

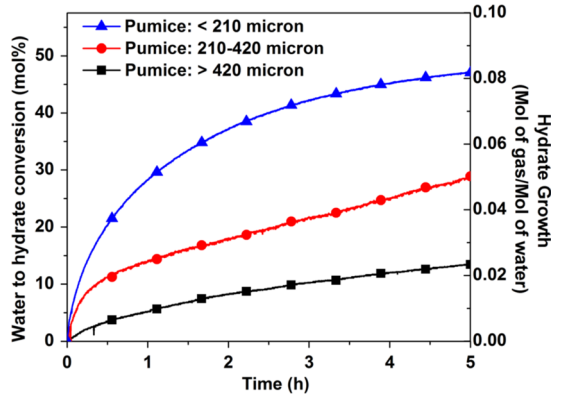


**Figure 4.** Effect of particle size of Pumice on hydrate formation kinetics. Pumice >420 $\mu$m, experiment number 14; pumice 210−420 $\mu$m, experiment number 17; pumice <210 $\mu$m, average of experiment numbers 20, 23 and 25.


DOI: 10.1021/acssuschemeng.5b00171
ACS Sustainable Chem. Eng. 2015, 3, 1205−1214

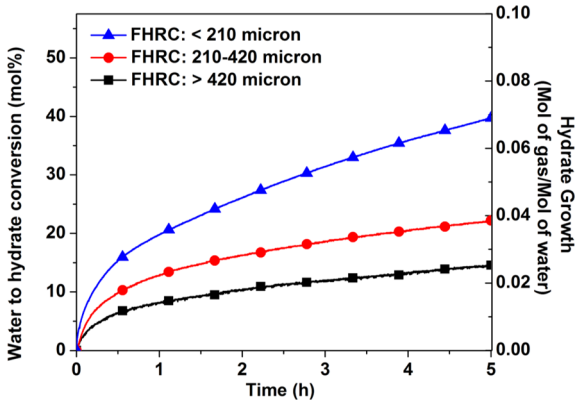


**Figure 5.** Effect of particle size of FHRC on hydrate formation kinetics. FHRC >420 $\mu$m, experiment number 26; FHRC 210–420 $\mu$m, experiment number 29; FHRC < 210 $\mu$m, average of experiment numbers 32, 35 and 37.

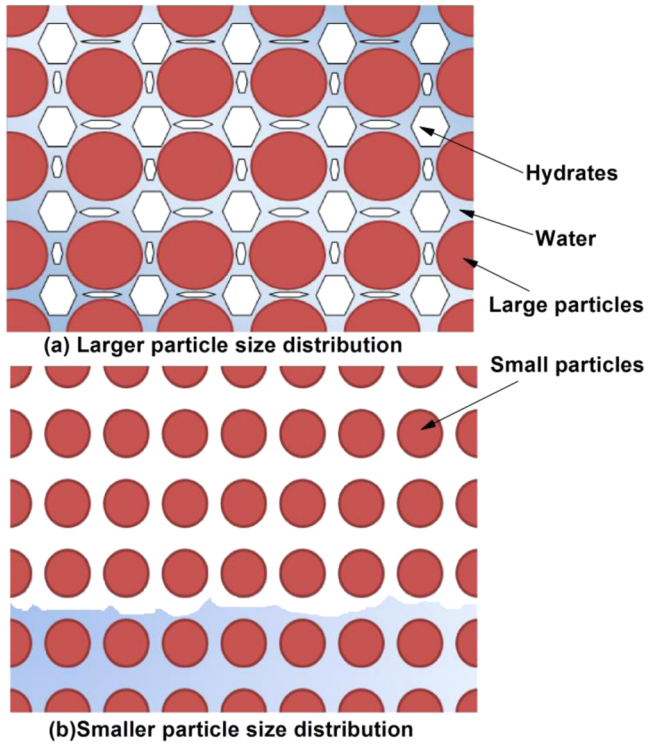


**Figure 6.** Mechanism of hydrate formation in systems having different particle size fractions. (a) Large particle size fraction: no interaction between the hydrates and the surface of the particles. (b) Small particle size fraction: hydrates form in large masses almost completely enveloping the particles themselves. (Maroon, sediment particles/grains; blue, water; white, hydrates).

conversion after nucleation with respect to time. It is to be noted that these experiments were all conducted with a constant volume of water (24 $cm^3$) and varying bed heights. As can be seen from the figures, hydrate formation kinetics is enhanced with decrease in particle size. These observations are in good agreement with those made by some earlier studies. Heeschen et al. reported a kinetic promoting effect of finer grain sizes of quartz sand on methane hydrate formation in methane–sand–water and methane–sand–seawater systems.[41] Mekala et al. studied the effect of particle size on $CO_2$ hydrate formation kinetics with a view on $CO_2$ sequestration using silica sand as the porous medium in the presence of both pure water and seawater.[42] They observed that a decrease in particle size enhances hydrate formation kinetics. Siangsai et al. investigated the effect of particle sizes of activated carbon on methane hydrate formation and dissociation. They speculated that compared to a system having only quiescent water, the presence of activated carbon particles increases the gas–water interfacial area by allowing the gas to pass through the carbon bed by making use of interstitial spaces present in the bed.[43] Babu et al. studied methane hydrate formation in the presence of porous media (activated carbon and silica sand). Their results showed that pore space and its corresponding interconnectivity play an important role in hydrate formation.[44] A smaller grain size ideally leads to a more regular packing and thus results in more interconnectivity of the pores and greater surface area for gas–water contact.[43,44] With the help of glass micromodels, Tohidi et al. observed the difference in mechanisms of formation of gas hydrates in sediments having different particle size fractions. Hydrate formation in the interstitial spaces between grains in the sediment occurs at the center of the pores rather than on the surface of the grains.[45,46] This is mainly due to the preferential wetting of the particle surfaces with water rather than gas. However, Tohidi et al. observed that this holds true mainly for large grain sizes (0.313 mm) whereas for the smaller grain sizes (0.070 mm), the hydrates form large masses almost completely encompassing the grains. This has been represented in the form of a well detailed schematic as Figure 6. We can thus conclude that decrease in particle size increases the surface area for gas–water contact. A larger surface area for gas–water contact means an increased number of nucleating sites thus resulting in accelerated hydrate growth.[41] The observation made in this study (enhancement in hydrate formation kinetics in the presence of small particle size fractions) is probably a combination of all these factors.

Gas–water interfacial area is an important aspect of hydrate formation kinetics and can be affected by a number of other factors too. The water saturation of the bed is one such dynamic that affects the contact area between gas and water. There are two scenarios: First, when the pores are completely filled with water and it cannot be replaced/moved by $CO_2$ pressure. In this scenario, hydrate formation will proceed through dissolution of gas into the water. In the second scenario, the pores are partially filled with water and thus under $CO_2$ pressure, these interconnected pores will have higher interfacial area of contact by creating a dedicated gas channel within the pores. This aspect of gas diffusion is further explored when conducting experiments with different bed heights. Averages of the gas uptake and the water to hydrate conversion for the repeat runs have been included separately in the Supporting Information as Figures S7 and S8, respectively. The rates of gas uptake corresponding to Figures 4 and 5 have been plotted against time and are present in the Supporting Information as Figures S9 and S10. As expected, the rate of gas uptake is the maximum for the smallest particle size fraction in the case of both pumice and FHRC.

**Effect of Bed Height on Gas Hydrate Formation Kinetics.** Figure 7 shows the effect of bed height on gas uptake and water to hydrate conversion for the hydrate formation experiments using pumice as the porous medium. Only the fresh runs have been included in Figure 7. Two different bed heights were taken: 2.7 and 5.5 cm. In the first case (2.7 cm), the volume of water used was 24 $cm^3$ whereas in the second


DOI: 10.1021/acssuschemeng.5b00171
ACS Sustainable Chem. Eng. 2015, 3, 1205–1214

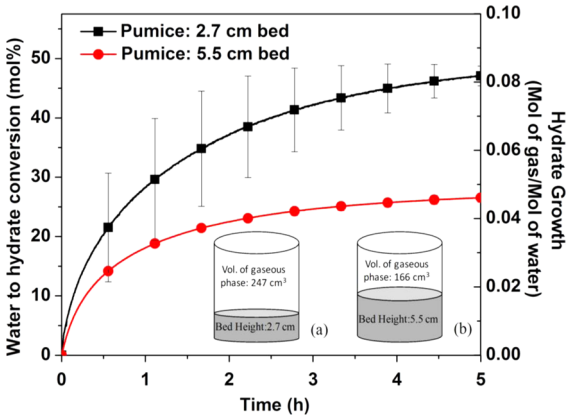


**Figure 7.** Effect of bed height on hydrate formation kinetics using pumice as the porous medium: pumice 2.7 cm bed, average and standard deviation of experiment numbers 20, 23 and 25; pumice 5.5 cm bed, average and standard deviation of experiment numbers 57, 60 and 62. (Inset) the different bed heights considered for the study and the corresponding change in volume of the gaseous phase: (a) bed height, 2.7 cm; (b) bed height, 5.5 cm.

case (5.5 cm), the volume of water used was 44.1 $cm^3$ (75% saturation in both cases). Further details are given in Table 3. A smaller bed height ensures efficient transfer of hydrate forming gases to the bottom of the reactor and thus enhanced rate of hydrate formation. It can be seen in Figure 7 that with increase in the bed height, water to hydrate conversion decreases as does the total gas uptake. This is probably due to the limited diffusion/migration of gas molecules deep inside the porous bed. This leads to the conclusion that bed height indeed affects the availability of sufficient gas to the water dispersed in the bed for hydrate formation. Extrapolating these results to real-world systems can give us important conclusions regarding the challenges to be faced when applying these schemes on a pilot/field scale. In a real-world system, there will always be enough bed height present, i.e., the porous geological formation would always limit the migration of gas molecules deep inside the bed. The results obtained in this study point to the fact that $CO_2$ sequestration in porous geological formations would be at a relatively lesser rate than those obtained through experiments performed in the laboratory. Averages of the water to hydrate conversion and the gas uptake for the repeat runs are given in the Supporting Information as Figure S11. The rates of gas uptake corresponding to Figure 7 have been plotted against time and are included in the Supporting Information as Figure S12. The system with the smaller bed height shows faster uptake of the gas.

**Hydrate Saturation.** Average hydrate saturation (%) obtained for different porous media (pumice and FHRC) are listed in the Supporting Information as Table S2. Hydrate saturation has been calculated only for the fresh runs. Hydrate saturation for our study ranges from 21.9% (pumice system with 44.1 $cm^3$ water and 5.5 cm bed height) to 37.5% (pumice system with 24 $cm^3$ water and 2.7 cm bed height). The hydrate saturation also decreases with increase in bed height. Sun and Englezos reported hydrate saturation for a silica sand system with water saturation of 25%.[14] They performed two types of experiments: injection of $CO_2$ in a gas cap and injection of $CO_2$ in a spiral tube mode. The water to hydrate conversion (mol %) for these experiments ranged from 38% to 55% for 24 h runs and was thus comparable with those obtained in the present study. The hydrate saturation for Sun and Englezos' study ranged from 10.7% to 15.2% whereas in the present study, it is observed to vary from 21.9% to 37.5%. The reason for this is the high initial water saturation level used in the present work (75%) compared to that in Sun and Englezos' study. On the basis of these results, we can conclude that the initial water saturation level too has a major role to play at least on the final hydrate saturation.

## CONCLUSIONS

Hydrate formation experiments were carried out in a fixed bed apparatus with a $CO_2$–water system and various porous media with a focus on geological storage of $CO_2$ in the form of gas hydrates. Four types of porous media were used: pumice, FHRC, silica sand and quartz. Two different types of experiments were carried out keeping (a) the volume of water used constant and (b) the height of the fixed bed constant. In both types of experiments, hydrate formation kinetics were found to be the most enhanced when pumice was used as the porous medium. The effect of particle size on hydrate formation kinetics was looked into. Pumice and FHRC were each divided into three size fractions. Kinetics was found to be enhanced greatly with decrease in particle size in the case of both pumice and FHRC. The effect of bed height on hydrate formation kinetics was also studied using pumice as the porous medium. Two different bed heights were chosen, 2.7 and 5.5 cm, to study the effect of gas diffusion/migration on hydrate formation kinetics. Rate of hydrate formation decreases with increase in bed height as a result of reduced gas diffusion/migration. Pumice and FHRC, used in this study, seem to be as good as silica sand or quartz in terms of kinetics of $CO_2$ hydrate formation as well as the water to hydrate conversion. Pumice and FHRC are typical volcanic sediments that are available in India and both these materials provide us with an option for geological storage of $CO_2$ in the form of gas hydrates.

## ASSOCIATED CONTENT

### Supporting Information

Volume of water required to completely fill the void spaces between the particles of the different size fractions of porous media used, the average hydrate saturation for different systems studied (Pumice and FHRC), figures plotting the average induction times in the presence of the different porous media studied, averages of the gas uptake and water to hydrate conversion for the repeat runs and the average rate of gas uptake for the fresh runs. The Supporting Information is available free of charge on the ACS Publications website at DOI: 10.1021/acssuschemeng.5b00171.

## AUTHOR INFORMATION

### Corresponding Author

*R. Kumar. Tel: +91 20 2590 2734. E-mail: k.rajnish@ncl.res.in.

### Notes

The authors declare no competing financial interest.

## ACKNOWLEDGMENTS

Authors gratefully acknowledge the financial support for this work from Council of Scientific and Industrial Research through 12th five year plan project (Project code: CSC 0102).



DOI: 10.1021/acssuschemeng.5b00171
ACS Sustainable Chem. Eng. 2015, 3, 1205–1214

## REFERENCES


(1) Kumar, R.; Linga, P.; Ripmeester, J. A.; Englezos, P. Two-stage clathrate hydrate/membrane process for precombustion capture of carbon dioxide and hydrogen. *J. Environ. Eng.* **2009**, *135*, 411−417.

(2) Lashof, D. A.; Ahuja, D. R. Relative contributions of greenhouse gas emissions to global warming. *Nature* **1999**, *344*, 529−531.

(3) Karl, T. R.; Trenberth, K. E. Modern global climate change. *Science* **2003**, *302*, 1719−1723.

(4) D'Alessandro, D. M.; Smit, B.; Long, J. R. Carbon dioxide capture: Prospects for new materials. *Angew. Chem., Int. Ed.* **2010**, *49* (35), 6058−6082.

(5) Aaron, D.; Tsouris, C. Separation of $CO_2$ from flue gas: A review. *Sep. Sci. Technol.* **2005**, *40*, 321−348.

(6) Miller, M. B.; Chen, D. L.; Xie, H. B.; Luebke, D. R.; Johnson, J. K.; Enick, R. M. Solubility of $CO_2$ in $CO_2$-philic oligomers; COSMOtherm predictions and experimental results. *Fluid Phase Equilib.* **2009**, *287* (1), 26−32.

(7) Sloan, E. D.; Koh, C. A. *Clathrate Hydrates of Natural Gases*, 3rd ed.; CRC Press: New York, 2008.

(8) Babu, P.; Kumar, R.; Linga, P. Pre-combustion capture of carbon dioxide in a fixed bed reactor using the clathrate hydrate process. *Energy* **2013**, *50*, 364−373.

(9) Kumar, A.; Sakpal, T.; Linga, P.; Kumar, R. Influence of contact medium and surfactants on carbon dioxide clathrate hydrate kinetics. *Fuel* **2013**, *105*, 664−671.

(10) Makogon, Y. F.; Holditch, S. A.; Makogon, T. Y. Natural gas-hydrates—A potential energy source for the 21st century. *J. Petrol. Sci. Eng.* **2007**, *56*, 14−31.

(11) Kumar, R.; Linga, P.; Moudrakovski, I.; Ripmeester, J. A.; Englezos, P. Structure and kinetics of gas hydrates from methane/ethane/propane mixtures relevant to the design of natural gas hydrate storage and transport facilities. *AIChE J.* **2008**, *54* (8), 2132−2144.

(12) Babu, P.; Kumar, R.; Linga, P. Unusual behavior of propane as a co-guest during hydrate formation in silica sand: Potential application to seawater desalination and carbon dioxide capture. *Chem. Eng. Sci.* **2014**, *117*, 342−351.

(13) Thomas, S.; Dawe, R. A. Review of ways to transport natural gas energy from countries which do not need the gas for domestic use. *Energy* **2003**, *28* (14), 1461−1477.

(14) Sun, D.; Englezos, P. Storage of $CO_2$ in a partially water saturated porous medium at gas hydrate formation conditions. *Int. J. Greenhouse Gas Control* **2014**, *25*, 1−8.

(15) Bickle, M. J. Geological carbon storage. *Nat. Geosci.* **2009**, *2* (12), 815−818.

(16) Bachu, S. Sequestration of $CO_2$ in geological media: Criteria and approach for site selection in response to climate change. *Energy Convers. Manage.* **2000**, *41* (9), 953−970.

(17) Haszeldine, R. S. Carbon capture and storage: How green can black be? *Science* **2009**, *325*, 1647−1652.

(18) Holloway, S. Underground sequestration of carbon dioxide—A viable green-house gas mitigation option. *Energy* **2005**, *30* (11), 2318−2333.

(19) Figueroa, J. D.; Fout, T.; Plasynski, S.; McIlvried, H.; Srivastava, R. D. Advances in $CO_2$ capture technology—The US Department of Energy's Carbon Sequestration Program. *Int. J. Greenhouse Gas Control* **2008**, *2* (1), 9−20.

(20) Koide, H.; Tazaki, Y.; Noguchi, Y.; Nakayama, S.; Iijima, M.; Ito, K.; Shindo, Y. (1992). Subterranean containment and long-term storage of carbon dioxide in unused aquifers and in depleted natural gas reservoirs. *Energy Convers. Manage.* **1992**, *33* (5), 619−626.

(21) Leung, D. Y. C.; Caramanna, G.; Valer, M. M. M. An overview of current status of carbon dioxide capture and storage technologies. *Renewable Sustainable Energy Rev.* **2014**, *39*, 426−443.

(22) Côté, M. M.; Wright, J. F. *Preliminary Assessment of the Geological Potential for Sequestration of $CO_2$ as Gas Hydrate in the Alberta Portion of the Western Canada Sedimentary Basin*; open file 6582; Geological Survey of Canada: Ottawa, ON, 2013.

(23) Mahoney, J. J. Deccan Traps. In *Continental Flood Basalts*; Macdougall, J. D., Ed; Springer Science and Business Media: Dordrecht, The Netherlands, 1988.

(24) Medlicott, H. B., & Blanford, W. T. *A Manual of the Geology of India: Chiefly Compiled from the Observations of the Geological Survey*; Oldham, R. D., Ed.; Cambridge University Press: New York, 2011.

(25) Subbarao, K. V.; West, W. D. *Deccan Volcanic Province, Volume 2*; Geological Society of India: Bengaluru, India, 1999.

(26) McPhie, J.; Doyle, M.; Allen, R. L. *Volcanic Textures: A Guide to the Interpretation of Textures in Volcanic Rocks*; CODES, University of Tasmania: Tasmania, Australia, 1993.

(27) Thomas, N.; Jaupart, C.; Vergniolle, S. On the vesicularity of pumice. *J. Geophys. Res.* **1994**, *99* (B8), 15633−15644.

(28) Venezia, A. M.; Floriano, M. A.; Deganello, G.; Rossi, A. Structure of pumice: An XPS and $^{27}$Al MAS NMR study. *Surf. Interface Anal.* **1992**, *18* (7), 532−538.

(29) Weems, J. B. Chemistry of clays. *Annu. Rep.—Iowa, Geol. Surv.* **1904**, *14* (1), 319−346.

(30) Lourenço, P. B.; Fernandes, F. M.; Castro, F. Handmade clay bricks: Chemical, physical and mechanical properties. *Int. J. Archit. Herit.* **2010**, *4* (1), 38−58.

(31) Herbert, J. A skill to build on: The brick-maker's art. *Ceres* **1994**, *145*.

(32) Martín-Barajas, A.; Lallier-Verges, E. Ash layers and pumice in the central Indian Basin: Relationship to the formation of manganese nodules. *Mar. Geol.* **1993**, *115* (3−4), 307−329.

(33) Iyer, S. D.; Sudhakar, M. Evidences for a volcanic province in the Central Indian Basin. *J. Geol. Soc. India* **1995**, *46*, 353−358.

(34) Sheth, H. C.; Ray, J. S.; Bhutani, R.; Kumar, A.; Smitha, R. S. Volcanology and eruptive styles of Barren Island: An active mafic stratovolcano in the Andaman Sea, NE Indian Ocean. *Bull. Volcanol.* **2009**, *71* (9), 1021−1039.

(35) Kumar, A.; Sakpal, T.; Roy, S.; Kumar, R. Methane hydrate formation in a test sediment of sand and clay at various level of water saturation. *Can. J. Chem.* **2015**, DOI: 10.1139/cjc-2014-0537.

(36) Kumar, A.; Sakpal, T.; Linga, P.; Kumar, R. Enhanced carbon dioxide hydrate formation kinetics in a fixed bed reactor filled with metallic packing. *Chem. Eng. Sci.* **2015**, *122*, 78−85.

(37) Linga, P.; Daraboina, N.; Ripmeester, J. A.; Englezos, P. Enhanced rate of gas hydrate formation in a fixed bed column filled with sand compared to a stirred vessel. *Chem. Eng. Sci.* **2012**, *68*, 617−623.

(38) Smith, J. M.; Van Ness, H. C.; Abbott, M. M. *Introduction to Chemical Engineering Thermodynamics*; McGraw-Hill Inc.: New York, 2001.

(39) Yang, S. H. B.; Babu, P.; Chua, S. F. S.; Linga, P. Carbon dioxide hydrate kinetics in porous media with and without salts. *Appl. Energy* **2014**, DOI: 10.1016/j.apenergy.2014.11.052.

(40) Natarajan, V.; Bishnoi, P. R.; Kalogerakis, N. Induction phenomena in gas hydrate nucleation. *Chem. Eng. Sci.* **1994**, *49*, 2075−2087.

(41) Heeschen, K.; Schicks, J. M.; Oeltzschner, G. The influence of sediment and fluid properties on methane hydrate formation. In *Proceedings of the 8th International Conference on Gas Hydrates*, Beijing, China, July 28−August 1, 2014.

(42) Mekala, P.; Busch, M.; Mech, D.; Patel, R. S.; Sangwai, J. S. Effect of silica sand size on the formation kinetics of $CO_2$ hydrate in porous media in the presence of pure water and seawater relevant for $CO_2$ sequestration. *J. Petrol. Sci. Eng.* **2014**, *122*, 1−9.

(43) Siangsai, A.; Rangsunvigit, P.; Kitiyanan, B.; Kulprathipanja, S.; Linga, P. Investigation on the roles of activated carbon particle sizes on methane hydrate formation and dissociation. *Chem. Eng. Sci.* **2015**, *126*, 383−389.

(44) Babu, P.; Yee, D.; Linga, P.; Palmer, A.; Khoo, B. C.; Tan, T. S.; Rangsunvigit, P. Morphology of methane hydrate formation in porous media. *Energy Fuels* **2013**, *27* (6), 3364−3372.

(45) Tohidi, B.; Anderson, R.; Clennell, M. B.; Burgass, R. W.; Biderkab, A. B. Visual observation of gas-hydrate formation and




DOI: 10.1021/acssuschemeng.5b00171
*ACS Sustainable Chem. Eng.* 2015, 3, 1205−1214

dissociation in synthetic porous media by means of glass micromodels. *Geology* **2001**, *29* (9), 867−870.
(46) Kuhs, W. F.; Chaouachi, M.; Falenty, A.; Sell, K.; Schwarz, J. O.; Wolf, M.; Enzmann, F.; Kersten, M.; Haberthür, D. In-situ microstructural studies of gas hydrate formation in sedimentary matrices. In *Proceedings of the 8th International Conference on Gas Hydrates*, Beijing, China, July 28−August 1, 2014.



DOI: 10.1021/acssuschemeng.5b00171
*ACS Sustainable Chem. Eng.* 2015, 3, 1205−1214